

## Detrapping of vacancies at $^{111}\text{In}$ in quenched silver

C. Alonso Arias, M. Behar, A. Filevich, and G. García Bermúdez\*

*Departamento de Física, Comisión Nacional de Energía Atómica, 1429 Buenos Aires, Argentina*

E. Savino

*Departamento de Metalurgia, Comisión Nacional de Energía Atómica, 1429 Buenos Aires, Argentina*

R. P. Livi and F. C. Zawislak

*Instituto de Física, Universidade Federal do Rio Grande do Sul, 90000 Porto Alegre, Brasil*

(Received 9 September 1980)

The isothermal recovery of a quenched Ag foil doped with  $^{111}\text{In}$  has been studied through the time-differential perturbed-angular-correlation technique. A nearest-neighbor-vacancy configuration has produced a quadrupole interaction frequency,  $\nu_Q = 166 \pm 3$  MHz, and a detrapping vacancy process has been detected with  $E_d = 1.09 \pm 0.05$  eV. The results are discussed and compared with previous measurements.

### I. INTRODUCTION

During the last few years hyperfine interaction methods have been extensively used in microscopic investigations of radiation damage in various metals. In particular, the time-differential perturbed-angular-correlation (TDPAC) technique has been applied to study the radiation damage in Ag (Refs. 1, 2) and Pd (Refs. 3, 4) doped with In impurities. In this kind of experiment equal numbers of vacancies and interstitials are produced; however, it has usually been assumed that vacancies were the trapped defects at the impurity site. No direct evidence of vacancy trapping was obtained in the above experiments; moreover, in Ref. 3 it was assumed that the trapped defects were interstitials.

In order to clear the controversy it seems important to perform measurements in systems where only one kind of defect is produced. For this purpose a quenching experiment appears to be a better approach.

In the present paper we report an experiment in which we have produced only vacancies or vacancy clusters, by first annealing and then quickly quenching an Ag foil. Then, using the TDPAC method and following the isothermal recovery of the Ag foil doped with radioactive  $^{111}\text{In}$  nuclei, we were able to measure the quadrupole frequency interaction at the  $^{111}\text{In}$  site and determine the detrapping vacancy energy. By comparing the present results with those published previously we are able to determine the nature of the trapped defects produced in Refs. 1 and 2.

The TDPAC measurements were performed through the well known 173–247-keV gamma-gamma cascade in  $^{111}\text{Cd}$ . The radioactive impurity nuclei of  $^{111}\text{In}$  (which populate nuclear levels of

$^{111}\text{Cd}$  by electron capture) were produced in the high-purity Ag matrix by using the alpha beam of the Buenos Aires Synchrocyclotron through the nuclear reaction  $^{109}\text{Ag}(\alpha, 2n)^{111}\text{In}$  (the estimated concentration of  $^{111}\text{In}$  in Ag is of the order of  $10^{-6}$ ). Then the samples were annealed at 1070 K in argon atmosphere, and quickly quenched by dropping into a bath of acetone cooled to 200 K.

### II. DATA ANALYSIS AND RESULTS

The analysis of the TDPAC data was made in the usual way, by extracting the perturbation factor

$$G_{22}(t) = \sigma_{20} + \sum_{n=1}^3 \sigma_{2n} \cos(\omega_n t) \exp(-\frac{1}{2} \delta \omega_n t), \quad (1)$$

where the various parameters are defined in Ref. 5. The frequencies  $\omega_n$  specify the nuclear quadrupole coupling constant  $\nu_Q$  and the asymmetry parameter  $\eta$

$$\nu_Q = \frac{eQV_{zz}}{h}, \quad \eta = \frac{V_{xx} - V_{yy}}{V_{zz}}.$$

Here  $V_{xx}$ ,  $V_{yy}$ , and  $V_{zz}$  are the principal components of the electric field gradient (EFG) and  $eQ$  is the electric quadrupole moment. The term  $\exp(-\frac{1}{2} \delta \omega_n t)$  in the expression (1) gives the Lorentzian distribution of frequencies having a width  $\delta \omega_n$ .

The experimental  $A_{22}G_{22}(t)$  curves in Fig. 1 show more than one frequency. As a consequence, the results were fitted with a function of the form  $G_{22}(t) = \sum_i a_i G_{22}^{(i)}(t)$ , where  $a_0$  is the fraction of probe nuclei which do not feel any hyperfine field and  $a_i$  is the fraction that feels the quadrupole interaction frequencies  $\omega_n^{(i)}$ . Each  $G_{22}(t)$  factor is given by the expression (1) and  $\sum_i a_i = 1$ .

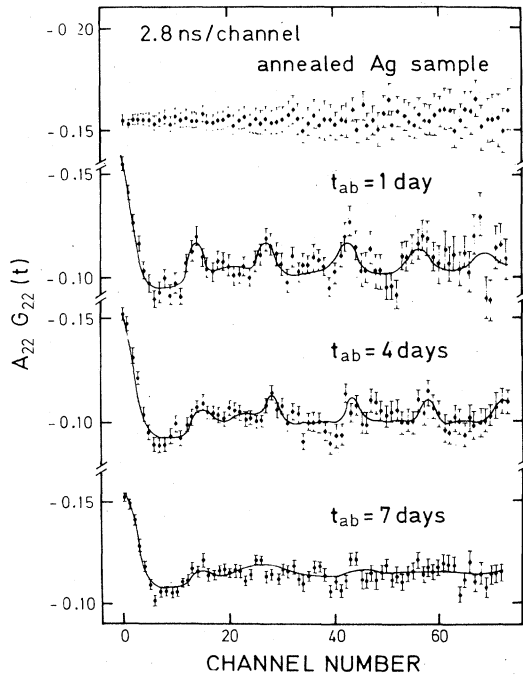


FIG. 1.  $A_{22}G_{22}(t)$  curves obtained at room temperature, for an annealed sample and 1, 4, and 7 d after the quenching.

The set of room-temperature measurements shown in Fig. 1 was performed as a function of the time  $t_{ab}$  elapsed since the fast quenching at 200 K up to the end of each measurement. The time required to obtain each  $A_{22}G_{22}(t)$  curve was 24 h; therefore the parameters presented in Table I are averages in this time. The quadrupole parameters obtained from the computer fittings of the  $A_{22}G_{22}(t)$  curves are shown in Table I. Also in Fig. 1 is shown the result for an annealed Ag sample after the alpha bombardment and before the quenching, which, as is expected, corresponds to the unperturbed  $A_{22}G_{22}(t)$  value. This result shows that the annealing procedure, following the alpha-particle bombardment, was effective in

removing any irradiation-induced defects.

The data obtained at room temperature show that the interaction is characterized by two quadrupole frequencies. The first one,  $\nu_1$ , is smeared out having an amplitude  $a_1$  and the second one,  $\nu_2$ , is well defined and has an amplitude  $a_2$ . In addition, there is a percentage  $a_0$  of the  $^{111}\text{Cd}$  nuclei which does not feel any electric field gradient (background).

A second set of measurements was performed with samples cooled at 80 K immediately after quenching at 200 K. The results of this experiment are also shown in Table I. The measured frequencies are, within the errors, the same as the ones observed at room temperature. However, at the beginning  $\nu_2$  presents a large distribution of frequencies ( $\delta_2 = 0.20$ ) which decreases with time becoming almost zero after  $t_{ab} = 9$  d. Finally, we observe that after  $t_{ab} = 9$  d, the parameters obtained from the fitting are very similar to those initially observed in the room-temperature measurement.

### III. DISCUSSION AND CONCLUSIONS

By comparing our results with those of Refs. 1 and 2 one can observe that for all the cases, in addition to a sharp quadrupole frequency, a second one appears, lower and with large dispersion. In the present work this frequency is centered around 100 MHz and in the previous experiments was a value near zero.

From our present theoretical and physical understanding of the TDPAC technique, we can only relate sharp quadrupole frequencies with lattice defects of well defined symmetry. Broad distribution of frequencies, though distinctively identified, can only be related to random distribution of defects around the probe, or lattice disturbance. Therefore it is rather difficult to infer from ill-defined frequencies any relevant defect information, and in the following we will confine our discussion to the behavior of the well-defined  $\nu_2$  quadrupole frequency.

Thermal quenching of the sample will partially

TABLE I. Parameters extracted from the fitting of  $A_{22}G_{22}(t)$  curves, measured at 300 and 80 K.

	$t_{ab}$ (d)	$a_0$ (%)	$a_1$ (%)	$\nu_1$ (MHz)	$\delta_1$	$a_2$ (%)	$\nu_2$ (MHz)	$\delta_2$
300 K	1	$55 \pm 2$	$29 \pm 2$	$106 \pm 3$	$0.25 \pm 0.05$	$16 \pm 1$	$166 \pm 3$	0.02
	3	$57 \pm 1$	$35 \pm 2$	$103 \pm 2$	$0.30 \pm 0.05$	$8 \pm 1.5$	$166 \pm 3$	0.01
	4	$57 \pm 2$	$37 \pm 3$	$100 \pm 3$	$0.32 \pm 0.06$	$6 \pm 2$	$160 \pm 3$	0.01
	7	$64 \pm 1$	$34 \pm 3$	$101 \pm 3$	$0.27 \pm 0.04$	$2 \pm 1$	$166 \pm 3$	0.01
80 K	1	$51 \pm 2$	$21 \pm 1$	$100 \pm 2$	$0.15 \pm 0.06$	$28 \pm 2$	$153 \pm 3$	0.20
	5	$52 \pm 2$	$24 \pm 2$	$100 \pm 2$	$0.40 \pm 0.06$	$24 \pm 3$	$160 \pm 3$	0.13
	9	$52 \pm 2$	$30 \pm 2$	$106 \pm 3$	$0.56 \pm 0.03$	$18 \pm 2$	$166 \pm 3$	0.04

confine the high-temperature vacancy concentration. Some thermal stress can also be produced, but certainly no significant interstitial population is expected to be found. Therefore the sharp and strong frequency interaction  $\nu_2$  observed at room temperature can be associated with the EFG produced by single-vacancy configurations trapped at a nearest-neighbor (NN) position to the  $^{111}\text{In}$  probe.

The results of Table I show evidence of vacancy detrapping processes, since the  $a_2$  population decreases and at the same time the  $a_0$  and  $a_1$  populations increase with the time  $t_{ob}$ . The detrapping energy can be calculated following the isothermal recovery of the sample. Assuming (a) that the change of  $a_2$  is due to single-vacancy detrapping, and (b) if there is more than one vacancy as NN of  $^{111}\text{In}$ , they interact weakly among themselves, one can use chemical rate theory. Then the amplitudes  $a_2$  related to the impurity defect complex can be written as

$$a_2 = a_2^0 \exp[-ft_{ob}z \exp(-E_d/kT)],$$

where  $a_2^0$  is the initial NN defect population,  $z$  is the number of combinations for the complex dissociation,  $f$  is the defect jump frequency ( $f = 10^{13} \text{ sec}^{-1}$ ), and  $E_d$  is the detrapping energy. Figure 2 shows a plot of  $\ln a_2$  as function of  $t_{ob}$  (note that all the points are shifted half a day to the left since each measurement is an average over 24 h). As can be observed, a straight line fits the experimental points very well and a value  $E_d = 1.09 \pm 0.05 \text{ eV}$  is obtained from the slope, assuming a value of  $z = 10$ . This assumption is not critical since a change of a factor of 100 in  $z$  will only produce a  $\Delta E_d = 0.1 \text{ eV}$  variation.

With respect to the second set of measurements, no annealing processes are expected to occur at 80 K. Since the annealing has exponential dependence on the temperature, a few seconds of the sample at 200 K (quenching temperature) are

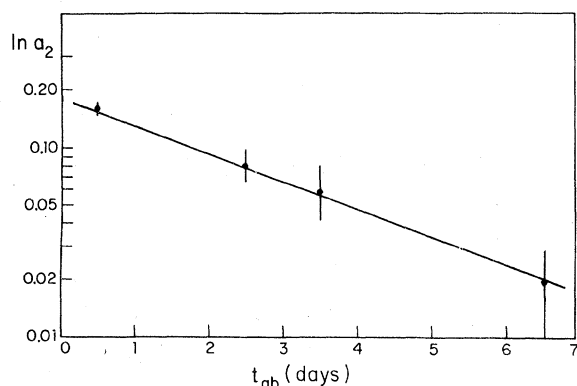


FIG. 2. Logarithmic plot of the amplitude  $a_2$  as function of the time elapsed after quenching (room-temperature experiment).

equivalent to almost infinite time at 80 K (measuring temperature). Table I shows, however, that for the measurements at 80 K, immediately after the quenching,  $\nu_2$  presents a large distribution, which decreases and approaches zero as the isothermal recovery time  $t_{ob}$  increases its value. After  $t_{ob} = 9 \text{ d}$ , not only  $\delta_2 \approx 0$  but also  $\nu_2$  reaches the value observed in the first set of measurements at room temperature. One explanation for this behavior is to assume that the sample is affected by thermal stress, by going from 200 to 80 K, and this stress relaxes after  $\approx 9 \text{ d}$ . If this is the case, the situation after 9 d has to be the same as the one observed at  $t_{ob} = 0$  for the room-temperature measurement. In fact, one can observe that the  $a_2$  population measured for  $t_{ob} = 9 \text{ d}$  at 80 K agrees very well with the population extrapolated for  $t_{ob} = 0$  at room temperature (see Fig. 2), giving further support for the above-mentioned idea.

By comparing the results of the present experiment with those of Behar and Steffen<sup>1</sup> and Thomé and Bernas<sup>2</sup> we can single out the following facts:

(a) The present high-frequency interaction  $\nu_2 = 166.0 \text{ MHz}$  is equal to the one measured in the experiment of Ref. 1,  $\nu_2 = 166.0 \text{ MHz}$  (note that in Ref. 1,  $\omega_2 = \nu_2/1.06$  is quoted).

(b) From Ref. 1 data, one can estimate the detrapping energy. The obtained value  $E_d = 1.12 \pm 0.03 \text{ eV}$  agrees fairly well with the present result of  $1.09 \pm 0.05 \text{ eV}$ . This is also the case of Ref. 2 where  $E_d = 1.17 \pm 0.2 \text{ eV}$  is obtained.

From all the above facts we can conclude that vacancies are the basically trapped defects in the Ag radiation-damage experiments of Refs. 1 and 2. Moreover, since we have obtained the same  $\nu_2$  frequency as in the experiment of Ref. 1, in both cases the same vacancy configuration has been produced. This is not the case of Ref. 2 where  $\nu_2 = 87 \text{ MHz}$  was the measured quadrupole frequency interaction. The presence of different NN vacancy configurations in different experiments is not unusual since in the same experiment,<sup>2</sup> by changing the temperature, the frequency dropped to 37 MHz indicating a rearrangement of the defect configurations. On the other hand, if 87 MHz is the frequency generated by a single vacancy, then 166 MHz would correspond to the one created by two vacancies situated in opposite sites with respect to the  $^{111}\text{In}$  probe (see Ref. 6).

Finally, it is interesting to note that different amounts of vacancy clustering, and different kinds of vacancy clusters can be found with different quenching temperature rates. More systematic work on this subject is needed, changing not only the quenching rate but also the temperature of measurement.

\*Work supported in part by the Consejo Nacional de Investigaciones Científicas y Técnicas, Buenos Aires, Argentina.

<sup>1</sup>M. Behar and R. M. Steffen, Phys. Rev. C 7, 788 (1973).

<sup>2</sup>L. Thomé and H. Bernas, Hyp. Int. 5, 361 (1978).

<sup>3</sup>H. Bertschat, H. Haas, F. Pleiter, E. Recknagel, E. Schloder, and B. Spellmeyer, Phys. Rev. B 12, 1 (1975).

<sup>4</sup>R. Butt, H. Haas, T. Butz, W. Mansel, and A. Vasquez, Phys. Lett. 64A, 309 (1977).

<sup>5</sup>H. Frauenfelder and R. M. Steffen, in *Alpha-, Beta-, and Gamma-Ray Spectroscopy*, edited by K. Siegbahn (North-Holland, Amsterdam, 1966), Vol. 2, p. 1101.

<sup>6</sup>J. A. H. da Jornada, I. J. R. Baumvol, M. Behar, R. P. Livi, and F. C. Zawislak, Hyp. Int. 5, 219 (1978).